GEOTHERMAL TRAINING PROGRAMME
Orkustofnun, Grensasvegur 9,
IS-108 Reykjavik, Iceland

Reports 2012
Number 6

FEASIBILITY STUDY OF DEVELOPING A BINARY POWER PLANT IN THE LOW-TEMPERATURE GEOTHERMAL FIELD IN PUGA, JAMMU AND KASHMIR, INDIA

Farooq Ahmed Ahangar
J&K State Power Development Corporation
Hotel Shaw Inn Boulevard Road
Srinagar-190001, J&K
INDIA
farooq.ahangar@yahoo.com

ABSTRACT

In the last few decades the binary power cycle, utilising the organic Rankine cycle (ORC), has become a preferred means for exploiting low- to moderate-enthalpy geothermal resources. Over the years the basic ORC has been improved and modified to better adapt the cycle to various conditions of the heat source. Presently, India, which has been exploring its geothermal resources for the last four decades, is considering the binary power cycle for exploiting one of its geothermal fields for electricity production and direct uses. This low-temperature geothermal field is located in the Puga Ladakh region of Jammu and Kashmir State in the northern part of India. This paper presents a feasibility study for developing a model binary power plant using the thermal energy of the brine of this field. The binary power cycle consists of a preheater, an evaporator, a superheater, a turbine-generator, a condenser, a recuperator and a feed pump. The choice for selecting the working fluid is restricted by the well-known harmful effects of CFCs which demand the adoption of either hydrocarbons or some new fluids. In the present paper, five working fluids (isobutane, n-butane, isopentane, n-pentane and propane) were considered for the model to obtain the optimum net power output. A thermodynamic model of a binary power plant using an air cooled condenser was created in the Engineering Equation Solver (EES) software. All the working fluids selected were run in the EES programme, assuming a well enthalpy of 900 kJ/kg and a mass flow rate of 150 kg/s.

1. INTRODUCTION

India is a country with about 1.22 billion people, accounting for more than 17% of the world's population. India, the second largest populated country after China, is a significant consumer of energy resources. It consumes its maximum energy in residential, commercial and agricultural purposes in comparison with China, Japan, Russia and the U.S. In recent years the availability of power in India has both increased and improved but demand has consistently outstripped supply. In India most of the power generation is carried out by using conventional energy sources, i.e. coal and mineral oil-based power plants, which contribute heavily towards greenhouse gases emissions. The setting up of new power plants is inevitably dependent on the import of highly volatile fossil fuels. Thus, it is essential to tackle the energy crisis through judicious utilization of abundant renewable energy resources, such as biomass energy, solar energy, wind energy, geothermal energy and oceanic energy.

In today's energy crisis, it has become very important to utilise the hot waste energy as an alternative energy source in order to meet energy demands. India is one of the Asian countries which has geothermal energy resources, but the utilization of this energy is still to be achieved. In India, systematic and comprehensive efforts to explore the geothermal energy resources by the Geological Survey of India started in early 1973 with the launch of the Puga geothermal project. Gradually the exploratory work was extended to cover the Chhumathang, Ladakh, J&K; Parbati valley, Himachal Pradesh; Sohana, Haryana; West coast, Maharashtra and Tattapani, Sarguja, Chhattisgarh (GSI, 2008). As a result of these surveys, 340 hot springs have been identified throughout the country. These springs are perennial and most of them can be utilised for direct thermal applications. Only some of them are suited for electrical power generation.

The hot springs present in the country are grouped into seven provinces, i.e. Himalayan province, Sohana province, Combay basin, Son Narmada lineament belt, West Coast province, Godavari basin and Mahanadi basin (MNRE, 2008) as shown in Figure 1. Among these, the Himalayan belt forms the most important region from the viewpoint of potential geothermal energy. This belt has a unique reserve of geothermal potential. In fact, it has been estimated that about 70% of the country's geothermal potential lies in this province.

Experimental space heating has already been carried out at Puga by fabricating huts of (5×5×2.5) m size, heated with geothermal water, with the temperature maintained at 20°C. Puga geothermal fluid has also been used for the extraction of borax and sulphur. Experimental poultry and mushroom cultivation units were also successfully completed.

On an experimental basis, a 5 MW technology demonstration power plant is being installed in Puga, geothermal field through a private developer. The installation of the country's first geothermal power plant was conceived with the objective of obtaining baseline information on geothermal power development which may be of great use for planning the harnessing of geothermal resources in Himalayan province and other parts of the country. The utilization of the geothermal energy source in this region shall provide clean energy for lighting, space heating, spas, industrial use and green house farming and shall improve the local people's living standards.

2. STUDY DESCRIPTION

2.1 Focus of the work

For low- to medium-temperature resource utilization, binary power plants are the best solution for converting waste heat into useful electrical power. In low-temperature regions, it is not possible to install steam turbines; however, a binary power plant based on the organic Rankine cycle using organic fluid as a working fluid has proved to be a good way to recover heat from a lower temperature heat source. Binary power plants, which have been cheerily described as "refrigerators running backwards", provide an appropriate technology for taking advantage of the thermal energy of brine or geofluid which is transferred to the low boiling working fluid through the heat exchanger to drive the turbine.

The focus of this project work is to model a binary power plant to achieve an optimum net power output on the basis of the available data.

2.2 Puga geothermal field – background information

Puga geothermal field, at an altitude of about 4400 m above mean sea level, is located in the north-west part of the Himalayas. Lying in the southeast part of Ladakh, the region of Jammu and Kashmir State, it forms a part of the Himalayan geothermal belt, with geographical co-ordinates 33°13´ North and 78°19´ East. The Puga area is surrounded by hills rising up to an altitude of about 6000 m, forming a valley. The area is about 700 km away from Srinagar city and about 190 km from Leh Town, the district headquarters. Puga valley, located in the northernmost area, as shown in Figure 1, is in the remotest and coldest part of the country and is about 15 km long with a maximum width of 1 km trending nearly east-west in direction between Sumdo village in the east and Pologongka La in the west. The geothermal activity, which is spread over an area of 5 km^2 is confined within the two N-S trending faults, namely Kaigar Tso fault to the west and Zildat fault to the east. The field, known to be the most promising geothermal field in the country, has an estimated capacity of 20-100 MW as indicated by the geoscientific studies in the area.

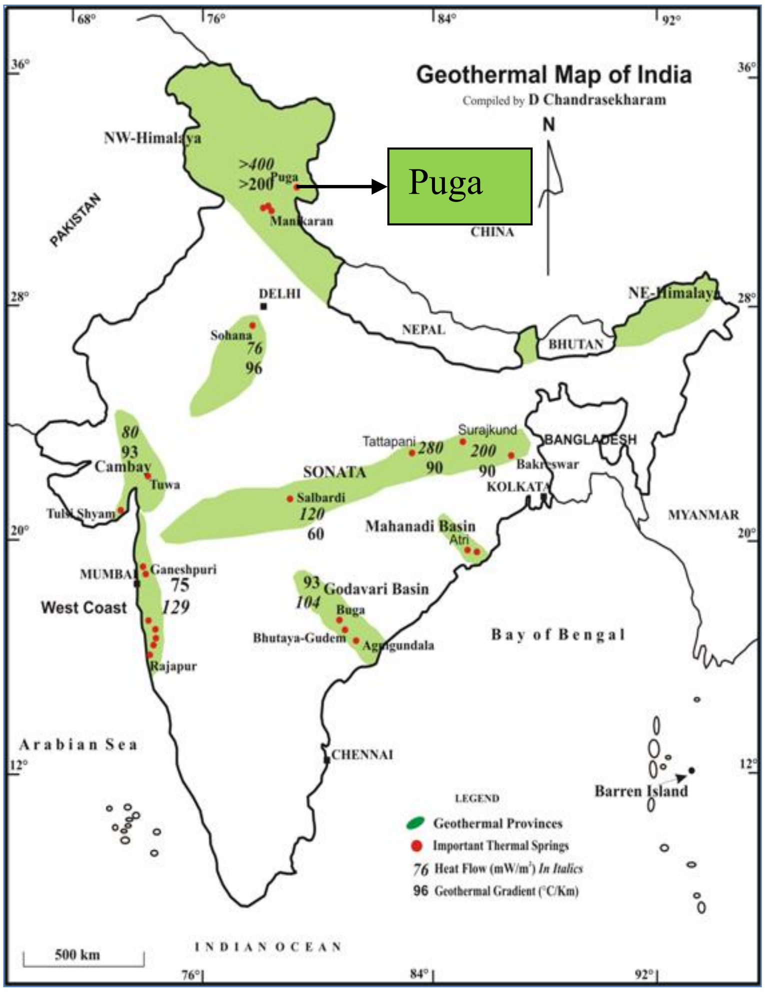

FIGURE 1: Geothermal provinces in India

2.2.1 Geological studies

The Puga geothermal area is located close to the colliding junction of the Indian and Eurasian plates which were involved in the Himalayan Orogeny. The area has been divided into the northern, the central and the southern tectonic belts. The northern belt exposes a thick sequence of sediments of shallow marine to fluvial origins, called the Indus group, deposited over the older granite basement. These rocks range in age from Cenomanian to Miocene and are intruded by young granite. The contact between the Indus group and the central belt comprising a ophiolitic suite is tectonic along Mahe fault. The Chhumathang geothermal field is located in this belt.

The central belt or the Indus Suture zone (ISZ) represents the remnants of the uplifted wedge of the oceanic crust which is now compressed between two continental masses. This belt, with a width of 3-5 km and trending NW-SE, consists of basalt (pillow lava), ultrabasic rocks, tuffs, agglomerate and associated sedimentary rocks. No geothermal activity is seen in this belt.

The southern belt exposes gneiss, schist and phyllite, interlayered with bands of limestone. There are indications that these rocks overlie a granite basement. These are intruded by at least two phases of younger granites. The Puga geothermal field, as can been seen in the Figure 2, is situated in this belt.

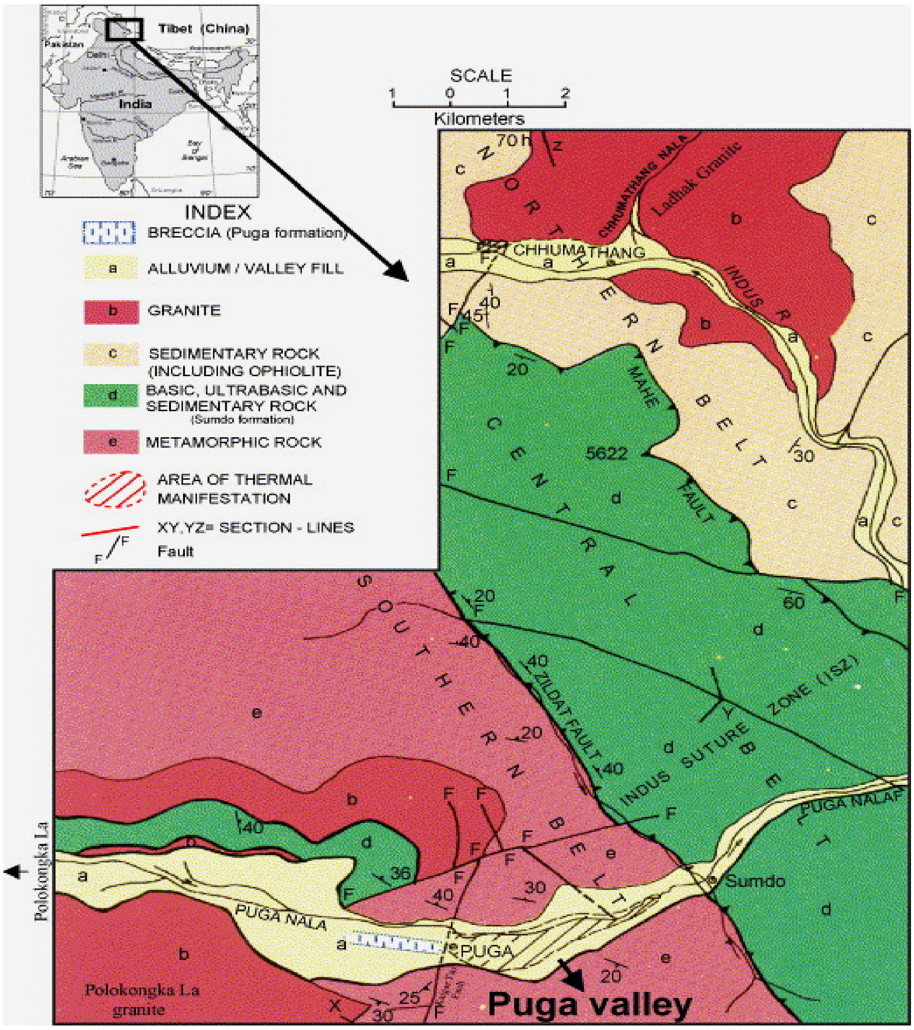

FIGURE 2: Geological and tectonic map of Puga and surrounding region (Harinarayana et al., 2004)

Zildat fault, representing the northern limit of the Indian plate, defines the southwestern limit of the ISZ. Puga is located to the west of the ISZ. Zildat fault practically defines the eastern limit of the geothermal system, at least in terms of surface manifestations. Just west of the area of thermal manifestations, Kiagar Tso fault crosses the valley and broadly delimits the thermally anomalous area on the western side. Thus, a rather unique feature of the Puga geothermal system is that it is fault-bounded.

2.2.2 Geophysical surveys

Though all conventional geophysical surveys have been carried out in Puga valley since 1973, D.C. resistivity measurements using bipole-dipole and dipole-dipole mapping techniques and AMT surveys have, in particular, provided some very valuable information. Resistivity surveys have identified the western extremity of the conductive zone, which coincides with the Kiagar Tso Fault. Moreover, it has been clearly determined that the geothermal system does not extend vertically to much deeper levels below the valley. The interpreted geothermal zone in the valley extends to about 200 m in the western part and is even shallower in the eastern part (Mishra et al., 1996). AMT surveys based on 75 soundings for frequencies of 20 Hz and above, in both N-S and E-W orientations of electric dipoles, revealed a very well defined low resistivity zone. This zone has N-S trend extending underneath the southern ridge bounding the Puga valley. It, however, spreads in an E-W direction in the valley (Ravi Shanker et al., 1999). The lowest recorded value of 1 ohm-m is confined to a very narrow N-S trending zone in the median part of the southern ridge. It may indicate an upflow zone or a major conduit (Absar, 1981).

AMT and resistivity data indicate that there is an extensive area underlain by formations with resistivity values varying up to 30 ohm-m. Within this 30 ohm-m area, values of < 5 ohm-m occupy an area of about 6.5 km^2, more than the geothermally anomalous area marked on the basis of surface manifestations in the valley. This low-resistivity zone is considered to be reflective of a shallow reservoir of hot thermal fluids and zones of hydrothermal alteration. The thickness of these low-resistivity formations varies from 50 m in the eastern part of the geothermal field to about 300 m in the southwestern part. The fractured or thermally altered bedrock is generally found on-top of a resistive basement rock, with high resistivity values, regarded as impervious bedrock, with poor storage capacity, though it may be hot. The highly resistive substratum generally lies between the depths of 100 to 220 m at different places and extends down to a depth of 500 to 800 m. At many places it has been seen that a narrow zone of low to moderate resistivity (20-200 ohm-m) extends to great depths, flanked by layers of infinite resistivity. Such narrow zones appear to be the channels along which hot thermal fluids migrate upwards from the deeper reservoir and get stored at shallow depth. These surveys indicate that the main reservoir, in all likelihood, occurs at a considerable depth underneath the southern ridge (GSI, 2008).

2.2.3 Geochemistry

Remarkable uniformity in the chemical composition of borehole and spring discharges is clearly a characteristic feature of the Puga geothermal system. Consistent abundances of non-reactive ions, such as Cl, B and F, provide unequivocal evidence for a single source of thermal discharges. Moreover, groundwater mixing at shallow levels is either trivial or the fluids have been thoroughly stirred up after dilution. The Puga fluid is relatively dilute (TDS ~2400 mg/l), HCO_3-Cl type water with an abundance of alkalis and rare alkalis. It has relatively high concentrations of SiO_2, B and F and has a molal Na/K of about 13. It is unique in having the highest relative concentration of Cs and being the only known geothermal fluid with Cs>Li (Ravi Shanker et al., 1999). The pH value of the water varies between 7.2 and 8.5.

Gases in the thermal discharge consist of CO, H_2S, NH, N, CH_4 and He, in the same order of abundance. CO_2 and He are 88 and 99 and 0.04 to 0.22%, respectively, of the total volume of gases collected. Empirical gas geothermometry gives temperatures of 175-205°C (Srivastava et al., 1996) for the latest equilibrium of gases. Minor elements such as Ba, Sr, Pb, Zn and Cu have been analysed in the Puga fluid, their average values being 0.2, 0.5, 1×10^{-3}, 4×10^{-2} and 5×10^{-3} mg/l, respectively (GSI, 2008)

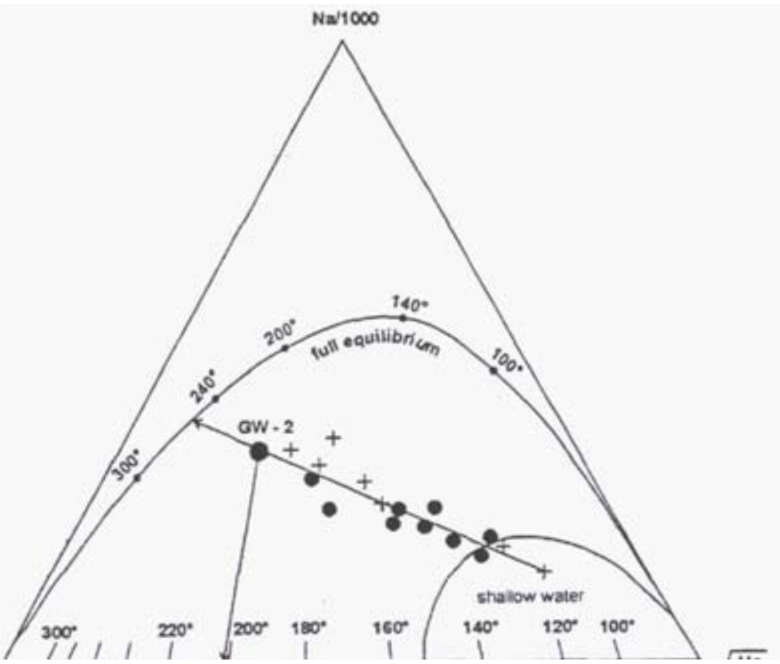

FIGURE 3: Na-K-Mg plot showing thermal discharges in various stages of partial equilibrium GW-2 discharge is the nearest representative of the Puga deep fluid, which has evidently Attained Na-K equilibrium at 255°C. The shallow reservoir temperature is indicated to be around 200°C (Ravi Shanker et al., 1999)

As Na, K and Mg ions are temperature dependent, a Na-K-Mg plot (Giggenbach, 1986) was used to get an idea about the reservoir temperatures at Puga (Figure 3). In spite of samples being in different stages of equilibration, a trend line was observed, which joins the least equilibrated samples with that of borehole GW-2. Discharge from GW-2 may be taken as the nearest representative of the deep equilibrated fluid with a temperature of 255°C. Taking fast equilibrating Mg into consideration, it is seen that GW-2 discharge is derived from a shallow reservoir at a temperature of about 200°C.

The single-phase deep fluid at a pressure of 45 bars, which includes P_{CO2} of 3.5 bars, gets cooled by conduction to a temperature of 200ºC during its ascent. This fluid then enters the valley through some N-S conduits.

2.2.4 Geohydrological studies

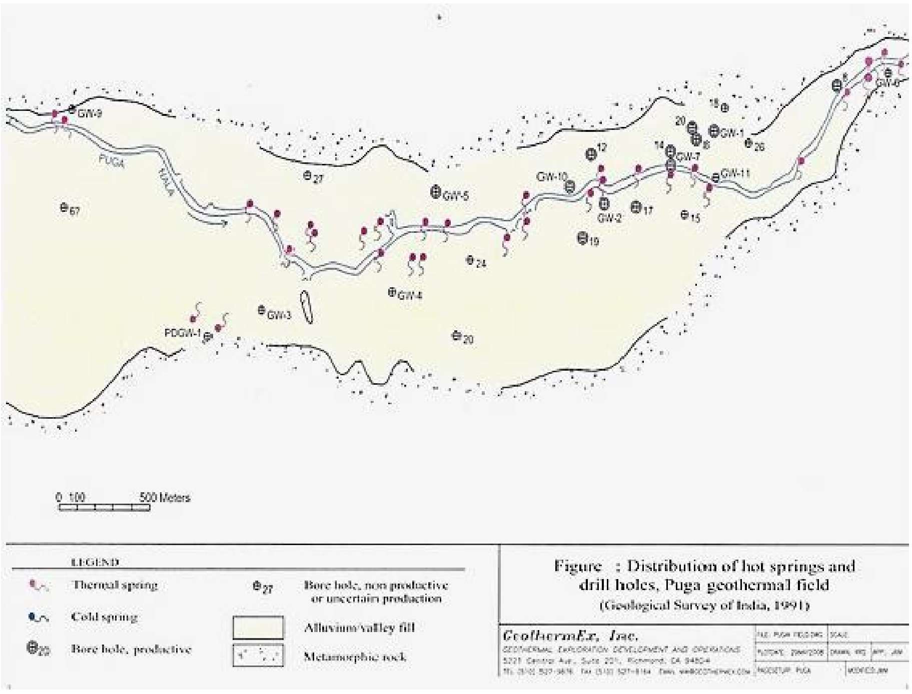

FIGURE 4: Hot spring and borehole locations in Puga area (MNRE, 2008)

These studies have indicated that the groundwater recharge is mainly from the snow-fed Puga-nalla river and its tributaries. Puga valley has a stream flowing through it as shown in Figure 4. This stream flows from west to east and is fed by Rulung glacier, located about 15 km west of Puga. In the major part of the area, except for a small stretch in the western part, no point in the valley is more than 1000 m away from the stream. In the eastern part, the distances are much smaller.

Flow from the stream is variable. When maximum in peak summer season, it is about 250 l/s. In the western part, the stream discharge is only about 25 l/s. During December – January, the stream is frozen on top with a meagre discharge of about 4-6 l/s.

There are two cold springs located in the western part of the area. These springs are the only source of drinking water in the area. Their discharge is about 25 l/s with TDS of 50 mg/l. Their discharge remains nearly constant year round. At the eastern end of the geothermal area, Puga stream has TDS of about 400 mg/l, comprising mainly Na, B, HCO_3, Cl and SO_4. It is, however, neutral to alkaline in pH and non-corrosive in nature.

2.3 Resource estimate

More than 100 hot springs have been observed in the Puga area with a temperature range of 30-84°C (84°C being the boiling temperature at this altitude). Maximum discharge from a single spring is about 15 l/s. Based on the resource assessment studies/surveys, a total of 34 boreholes with a depth range of 29-385 m have been drilled in Puga Valley. Many boreholes show geyser activity with steam and hot water mixture (as shown in Figure 5) but there are many boreholes with hot water only. Out of 34 drilled holes, 17 boreholes recorded geothermal artesian conditions with most of the wells constituting 10-15% steam. The highest bottom hole and discharge temperatures recorded are 140 and 130°C, respectively, with wellhead pressure varying from 2 to 3 kg/cm^2.

These 17 wells flowing wells, have a cumulative discharge of 83 l/s. Out of these 17 shallow flowing wells, eight good wells with an average enthalpy of 650 kJ/kg, as shown in Figure 6, exhibited a cumulative discharge of 53 l/s. Some wells discharged a water-steam mixture at 125ºC. The best well (GW-25) has a discharge of 8.3 l/s, wellhead temperature and pressure of 135°C and 3 bars, respectively. Most of the boreholes drilled ejected huge quantities of silica gel at the time of the first blow-out, implying that the SiO_2 temperature of 170°C may be on the low side.

Considering the geothermal gradient of 100-200°C/km (Ravi Shanker, 1988) and heat flow studies which indicated high heat flow values of about 540mW/m^2 in this region (Ravi Shanker et al., 1976), there is a high probability that temperatures above 200°C, possibly 230-250°C, may exist at about 1-2 km depth. On the basis of the reservoir temperature, it is estimated that the area has a potential for producing 20-100 MWe. The details of the Puga field are summarized in Table 1.

FIGURE 5: Geyser activity in a borehole at Puga

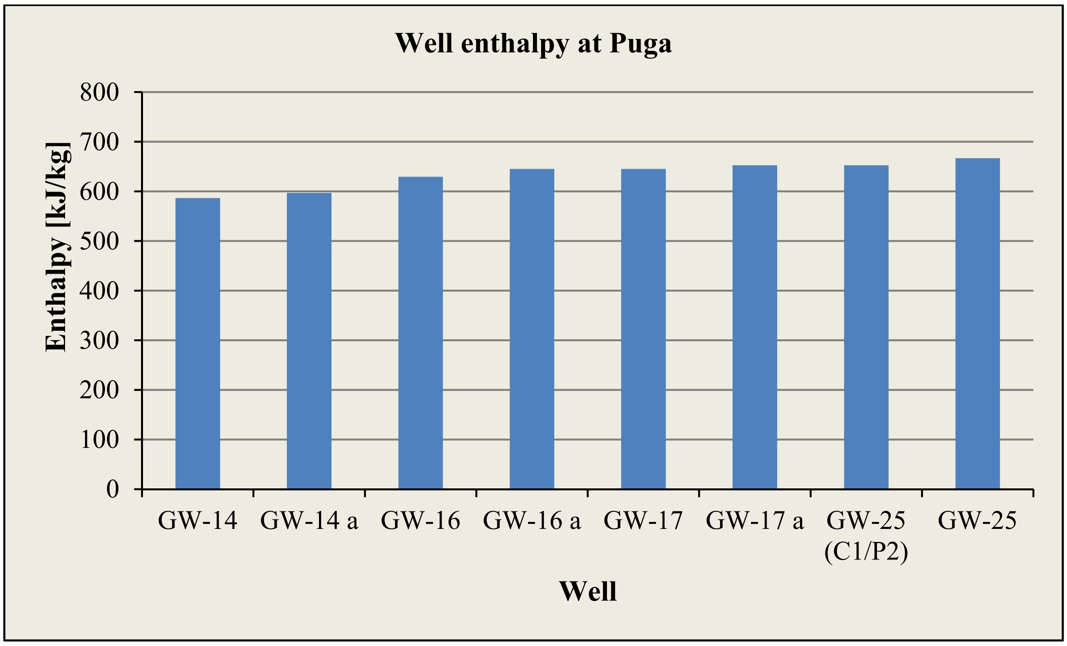

FIGURE 6: Enthalpy of eight good wells at Puga

TABLE 1: Details on Puga geothermal field

Parameter	Value
Area of Puga geothermal field	5 km^2
Total number of boreholes drilled	34
Productive wells	17
Cumulative discharge from 17 wells	83 l/s
Maximum depth achieved with a well	385 m
Maximum discharge from a single borehole	8.3 l/s
Estimated reservoir temperature	220-250 ºC
Maximum discharge pressure	2-3 bar
Steam content (of total discharge)	10-15%
Heat flow value	540 mW/m^2

2.4 Climatic conditions

Dry arctic climatic conditions prevail in the region and the active working period is restricted to about 5 months a year. Puga has distinct cold and warm seasons, like cold winters and warm summers. Temperature drops sharply at night. Winter has prolonged freezing periods, with the coldest month being January. The area experiences a good amount of snowfall during the winter. Snowfall may occur anytime between October and March. July is the warmest month with an average of 15°C at noon. January is the coldest month with an average temperature of -22 °C at night. November is, on average, the month with the most sunshine. Rainfall and other precipitation have no distinct peak month.

Relative humidity is very low, generally between 24 and 51%, the average value being around 30%. Precipitation is only about 150 mm, mainly in the form of snowfall. Massive continuous snowfall is rare. Rainfall is rare but there have been incidents of cloudbursts in the area around Puga during the recent past.

Wind speed in the valley varies from about 4 to >10 km/hr. Higher wind speed is recorded between the hours 14:00 and 20:00 when strong cold westerly winds prevail.

3. BINARY POWER CYCLE

The name ‘binary’ derives from the fact that two fluids are used in the power cycle. The primary fluid is the geofluid (brine) and the secondary fluid is the working fluid or power fluid.

Basically, there are two types of binary cycles, the organic Rankine cycle (ORC) and the Kalina cycle. If the geothermal fluid temperature is below 180°C, the ORC system is considered more economical, commonly using hydrocarbons as the appropriate working fluid. When the geothermal fluid (liquid water) temperature gets lower than 120-130°C, a Kalina cycle with a mixture of water-ammonia as the working fluid seems superior to the ORC cycle (Valdimarsson, 2011).

A binary system has two closed loop cycles; the first is the heat exchange cycle of the geothermal fluid and the second is the organic Rankine cycle for the working fluid. These two cycles are separated, so only the heat exchange takes place through the various heat exchangers which allows the heated geofluid to heat working fluid that has a lower boiling point than the geofluid. The working fluid, chosen for its appropriate thermodynamic properties, receives heat from the geofluid, evaporates and produces mechanical work in the turbine while expanding. The fluid is then discharged to the condenser where condensing heat is transferred to a cooling medium which is either water or air. The liquid condensate is then pumped at elevated pressure into the evaporator, completing the cycle.

In its simplest form, a binary power cycle follows the schematic flow diagram as shown in Figure 7. The main components of the basic binary power cycle are: heat exchangers (preheater, evaporator, condenser and regenerator), a feed pump, a turbine, a generator and a water or air cooled condenser.

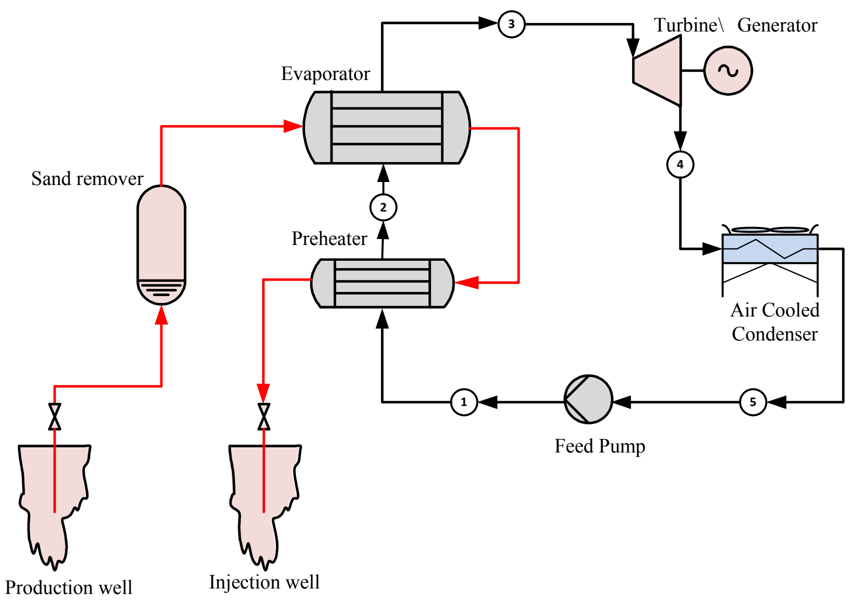

FIGURE 7: Schematic diagram of a basic binary cycle

Some of the benefits derived from a binary-cycle system include the ability to use a lower-temperature resource as well as a closed loop such that the geofluid is not lost and all geofluid is injected back into the ground. Binary cycle systems also reduce the likelihood of a build-up of calcium carbonate or other mineral scaling in the wells and/or turbines.

4. SELECTION OF WORKING FLUID

In designing the binary power cycles, selection of the working fluid is of prime consideration. There are several factors that have to be considered when selecting the working fluid. The proper choice of working fluid is of key importance as it has a major effect on the performance of the unit. Because of the low temperature of the heat source, irreversibilities occurring in heat exchangers are very harmful to the overall efficiency of the cycle. These inefficiencies are highly dependent on the thermodynamic properties of the working fluid.

The thermodynamic properties such as critical temperature, critical pressure, etc., of the working fluid strongly influence the performance of the system. These properties alone are not the only criteria to be taken into account during the selection of a working fluid; other key criteria include the impact of the working fluid on total system cost, health safety and environmental impacts. Because of their strong effect on ozone layer depletion, the use of fluorocarbons in such applications has been forbidden. The thermodynamic, environmental and health properties of some of the working fluids considered best for low-temperature reservoir binary plants are shown in Table 2 (DiPippo 2008). Pure water is included for comparison.

All the hydrocarbons are of retrograde type, which means that over some temperature ranges the slope of the water saturation line is positive. As proved by DiPippo (2008), fluids listed in Table 2 behave in that way over the whole range of temperatures typical for working fluids in geothermal binary cycles. This means that adiabatic expansion in the turbine will always have an effect in superheated vapour conditions at the turbine outlet.

TABLE 2: Properties of candidate working fluids

Fluid	Formula	Critical temp. (°C)	Critical pressure (bar)	Toxicity	Flamma-bility	ODP	GWP	Molecular wt.
i-Butane (iC4)	i-C_4H_{10}	134.9	36.85	Low	Very high	0	3	58.12
n-Butane (nC4)	C_4H_{10}	152.0	37.18	Low	Very high	0	3	58.12
i-Pentane (iC5)	i-C_5H_{12}	187.8	34.09	Low	Very high	0	3	72.15
n-Pentane (nC5)	C_5H_{12}	193.9	32.40	Low	Very high	0	3	72.15
Propane (C3)	C_3H_8	96.6	42.36	Low	Very high	0	3	44.10
Water	H_2O	374.14	220.89	Non-toxic	Non-flam.	0	-	18.0

There are three types of working fluids, i.e. dry fluids, wet fluids and isentropic fluids. A dry fluid has a positive slope of the saturation curve on a T-S diagram; a wet fluid has a negative slope; and an isentropic fluid has an infinitely large slope. Generally, dry and isentropic fluids are better working fluids for power plants based on organic Rankine cycle because they do not condensate after the fluid goes through the turbine.

Clearly all the fluids shown in Table 2 have critical temperatures and pressures far lower than water. The working fluid must be selected according to its critical temperature, which must be suitable for the temperature level of the geothermal fluid. The proper selection of a working fluid can significantly reduce the cost of a project and will have great implications on the performance of a binary plant. There is a wide selection of organic fluids that could be used in these cycles.

5. DESIGN OF BINARY POWER CYCLE WITH REGENERATOR

Using the boundary conditions and assumptions listed in Sections 5.1 and 5.2, the model of a binary power plant using a recuperator and a super-heater was created using Engineering Equation Solver (EES) software (F-Chart Software, 2012). The proposed model was run on different selected working fluids with the objective to obtain a maximum net power output.

Though 34 wells have been drilled in Puga geothermal field, the majority of these wells are of shallow depth. In the development of the Puga field, drilling of wells will be carried out to a depth of about 2000 m which would help in ascertaining the existence and viability of the deep reservoir. As mentioned in Section 2.3, heat flow studies indicated high heat flow values of about 540 mW/m^2 in this region; the field has a potential of about 230-250°C reservoir temperature at a depth of about 1000-2000 m.

Eight good wells out of 17 productive wells exhibited 10-15% of steam content. In order to be on the safe side, a well enthalpy of 900 kJ/kg was selected, which corresponds to approximately 200°C reservoir temperature. This enthalpy value is most likely on the safe side, and can be seen as an average between the proven well enthalpy and projected enthalpy from deeper wells.

5.1 Boundary conditions

The boundary conditions for the proposed model are:

- Assumed mass flow rate = 150 kg/s
- Well head pressure = 3 bar
- Steam content = 15% of total discharge
- Assumed well enthalpy = 900 kJ/kg
- Pressure drops and heat losses in the system are neglected.

Optimistic estimate: As more wells are to be drilled at Puga to a depth of about 2000 m, the estimated reservoir temperature, pressure and enthalpy could be higher as has been indicated by the geoscientific studies in the area. Wellhead pressure will most likely be higher for the high-reservoir temperatures of 250°C which corresponds to enthalpy of around 1100 kJ/kg and wellhead pressure of 10 bar-abs.

5.2 Assumptions

The assumptions made for the model are:

- Isentropic efficiency of turbine (η_t) = 85%
- Efficiency of pump (η_p) = 75%
- Ambient temperature = 10 ºC

The values assumed for the overall heat transfer coefficient (U) of heat exchangers (Páll Valdimarsson, pers. comm.) are:

U = 1600 W/m^2°C for evaporator or vaporiser;
U = 1000 W/m^2°C for preheater;
U = 600 W/m^2°C for superheater;
U = 400 W/m^2°C for recuperator;
U = 800 W/m^2°C for air cooled condenser; and
U = 400 W/m^2°C for the superheater.

5.3 Power cycle and working fluid

The proposed binary cycle power plant follows the schematic diagram shown in Figure 8. It consists of a separator, a preheater, an evaporator, a superheater, a turbine-generator, a recuperator, an air-cooled condenser and a feed pump. The working fluid operates in a sealed, closed loop cycle shown by a black line in the diagram. The thermodynamic process undergone by the working fluid is shown in Figures 9 and 10, in a temperature-entropy diagram and a pressure-enthalpy diagram, respectively.

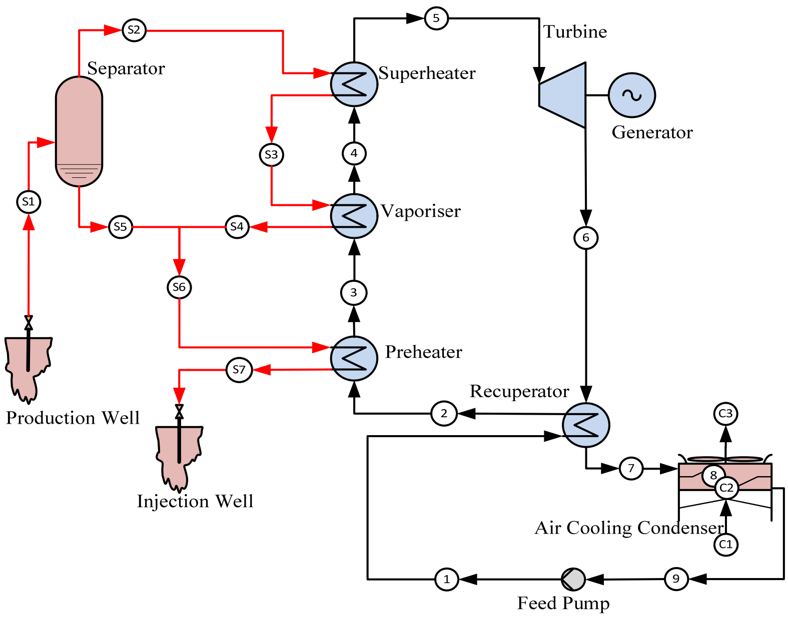

FIGURE 8: Schematic diagram of proposed binary plant with air cooling system

The stream of geothermal fluid from the well, indicated by a red line, enters the system through a network of heat exchangers (superheater, evaporator and preheater where heat is transferred to the working fluid. Typically (in a basic binary cycle), there are two stages of heat exchange: one occurring in a preheater, where the temperature of the working fluid is raised to a bubble point and the other in an evaporator, where the working fluid is vaporised.

However, in this proposed power cycle the fluid is brought to a superheated state by adding a third heat exchanger - superheater. After isobaric heat addition, which occurs between states 1 and 5, high-pressure vapour is expanded in the turbine from state 5 to state 6. The exhaust vapour of the organic fluid from this process is superheated, which is a result of the characteristic retrograde shape of the working fluid saturation line.

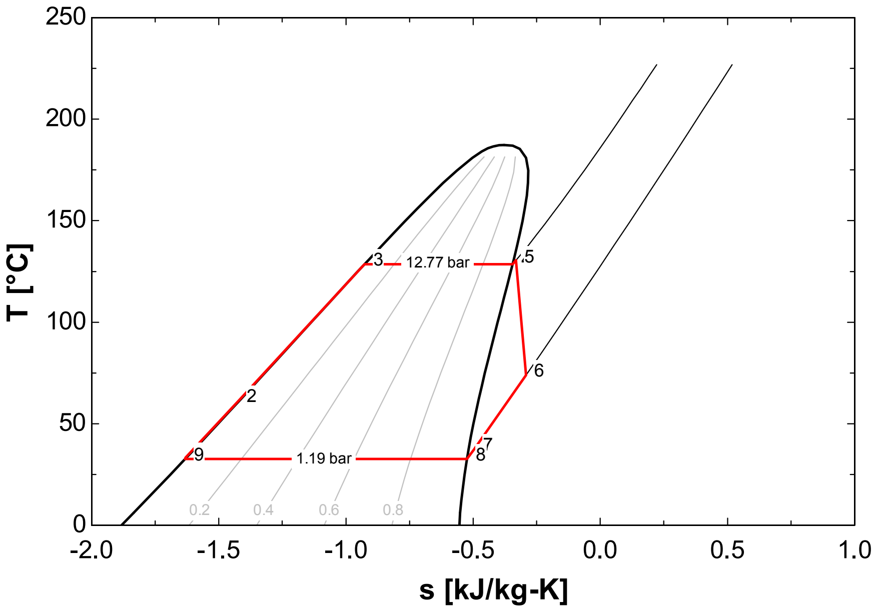

FIGURE 9: T-S diagram for model binary cycle

The superheated stream of exhaust vapour may be sent directly to the condenser, where it is cooled to temperature T_9 and is then condensed. However, the exhaust from the turbine is lead to another heat exchanger - recuperator which recovers part of the sensible heat of superheated vapour and transfers it to the stream of liquid working fluid entering the preheater. After leaving the condenser, the working fluid enters the pump, where its pressure is increased from P_9 to P_1 and returned through the recuperator to the preheater.

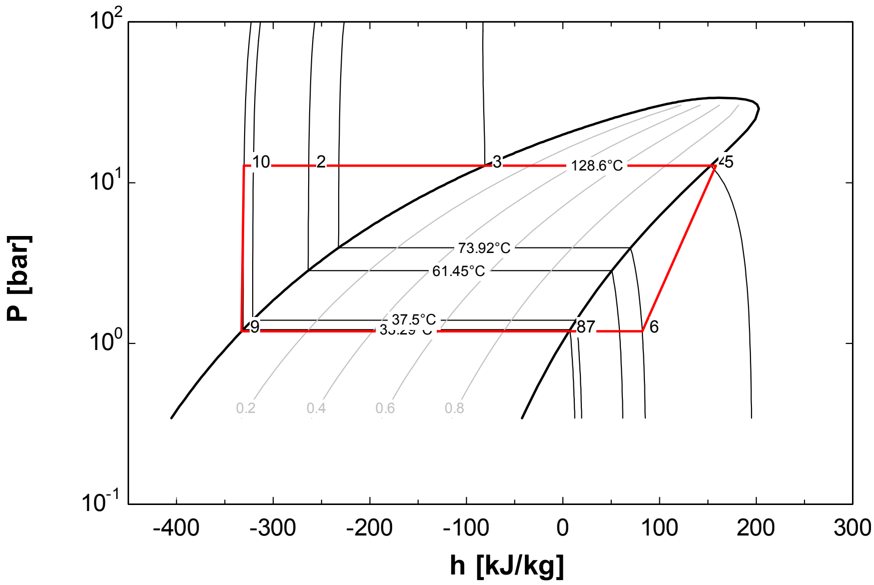

FIGURE 10: P-h diagram for model binary cycle

5.4 Plant components

The functions and the heat transfer equations related to each component of the proposed binary power cycle are described below:

5.4.1 Separator

The main thermal parameter for the geothermal reservoir, with regard to the power plant, is the field enthalpy or the energy content of the field. The steam-water enters into the separator as shown in Figure 11 at station s1. Station s2 is the steam outlet and station s3 is the brine outlet of the separator. In this study, the brine obtained from the wells has 10-15% of steam present.

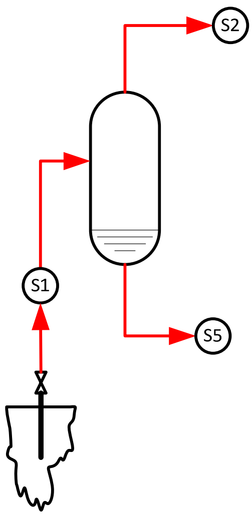

FIGURE 11: Separator

The wells have certain productivity, i.e. there is a relationship between the wellhead pressure and the flow from the well. The productivity varies from well to well. This relationship is further complicated by the fact that the well may not be artesian, that is well pump is required to get the fluid from the well. Generally, this relationship can be presented as below, where the function takes the presence of a well pump into account, as well the field characteristics:

$$\dot{m}_{well} = f(p_{s1}) \tag{1}$$

where $\dot{m}_{well}$ = Mass of the geothermal fluid at the wellhead;
p_{s1} = Pressure of the geothermal fluid at station s1.

The flow up the well and in the geothermal primary system can be usually treated as isenthalpic, that is the heat loss in the well and the piping is neglected. No fluid loss is assumed, therefore:

$$\dot{m}_{s1} = \dot{m}_{well} \tag{2}$$

$$h_{s1} = h_{well} \tag{3}$$

where h_{well} = Enthalpy of the geothermal fluid in the well;
h_{s1} = Enthalpy of the geothermal fluid at the wellhead.

The throttling in the well and primary system results most frequently when the fluid starts to boil; in that case the temperature is the direct function of the separator pressure (station s1). If the well is non-artesian and a well pump is used, the pressure may be sufficiently high to avoid boiling. In that case, the separator is not required at all and the source fluid is liquid and in the sub-cooled region all the time. If boiling occurs and a separator is employed, the relationship between temperature and pressure as given below is defined by the thermodynamic properties of steam and water:

$$T_{s1} = T_{sat}(p_{s2}) \tag{4}$$

The steam fraction is then defined by the energy balance over the separator. The heat flow in the incoming mixture of the steam and water (from the well) equals the sum of the energy flows in the steam and the brine from the separator. The mass flow of steam from the separator will then be:

$$m_{s2} = \dot{m}_{s1}\frac{h_{s1} - h_{s5}}{h_{s2} - h_{s5}} \tag{5}$$

The separator is working in the (thermodynamic) wet area, containing a mixture of steam and water in equilibrium. All temperatures in the separator will thus be equal, assuming that there are no significant pressure losses or pressure differences within the separator:

$$T_{s2} = T_{s1} = T_{s5} = T_{sat}(p_{s2}) \tag{6}$$

The separator pressure is:

$$h_{s5} = h_g(p_{s2}) \tag{7}$$

where h_g = Enthalpy of the geothermal fluid.

Mass balance for the separator, the sum of the steam and brine mass flowing out of the separator equals the mass flow of the mixture from the wells towards the separator:

$$\dot{m}_{s5} = \dot{m}_{s1} - \dot{m}_{s2} \tag{8}$$

5.4.2 Superheater

In the superheater the hottest geothermal fluid exchanges heat with the working fluid to bring the working fluid from a saturated state to a superheated state. The temperature difference between the

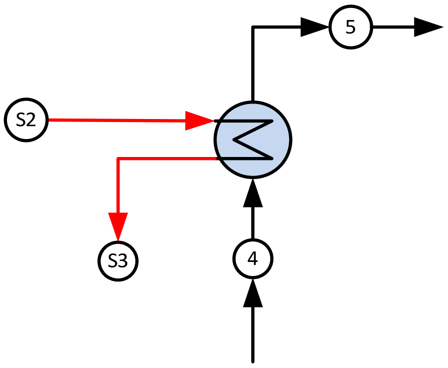

FIGURE 12: Superheater

entering geothermal fluid and the leaving working fluid is defined as the “approach to the heat exchanger”.

The super heater is the first component of this binary cycle as shown in Figure 12. Station s2 is the entry of the geothermal fluid to the superheater and station s3 is the outlet. Station 4 is the entry of the working fluid (vapour) to the superheater and station 5 is the outlet of the working fluid (superheated vapour) towards the turbine.

The heat removed from the geothermal fluid has to be equal to the heat added to the working fluid.

$$(\dot{m}_{s2}(h_{s2} - h_{s3}) = \dot{m}_{fluid}\,(h_5 - h_4\,) \tag{9}$$

where m_{fluid} = Mass of working fluid.

The fluid condition at station 5 is determined by the cycle and the turbine requirements, in the binary cycle shown at Figure 8; the fluid state is superheated as is shown in the T-s diagram in Figure 9.

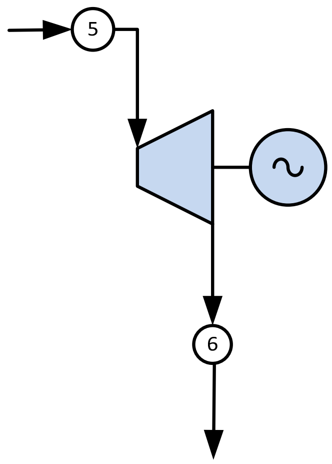

FIGURE 13: Turbine

5.4.3 Turbine

The turbine converts a part of the vapour enthalpy to the mechanical (shaft) work and then into electricity in the generator as shown in Figure 13. Station 5 is the entry point of the superheated vapour into the turbine and station 6 is the turbine exit.

The ideal turbine is isentropic, having no second law losses. In this case, the entropy of the incoming superheated vapour equals the entropy in the exhaust steam. The corresponding enthalpy change (reduction) of the vapour is the largest enthalpy change possible. The isentropic exit enthalpy is then the enthalpy at the same entropy as in the inlet and at the exit pressure, which is roughly the same as prevails in the condenser.

$$h_{6,s} = h(s_5, p_6) \tag{10}$$

The isentropic turbine efficiency is a known quantity, as the same is given by the turbine manufacturer. This efficiency is the ratio between the real enthalpy change through the turbine to the largest possible (isentropic) enthalpy change. The real turbine exit enthalpy (h_6) can then be calculated as:

$$\eta_t = \frac{h_5 - h_6}{h_5 - h_{6s}} \tag{11}$$

where η_t = Isentropic turbine efficiency which is assumed in this case to be 85%.

The work output of the turbine is then the real enthalpy change multiplied by the working fluid mass flow through the turbine:

$$\dot{W}_t = \dot{m}_{fluid}(h_5 - h_6) \tag{12}$$

where $\dot{W}_t$ = Power output of the turbine.

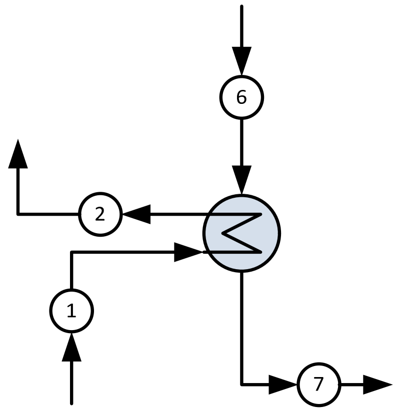

FIGURE 14: Recuperator

5.4.4 Recuperator

The recuperator, seen in Figure 14 (counter flow energy recovery heat exchanger) is located between the turbine exit and the condenser inlet. It is used to transfer the heat from the turbine exit vapour to the condensate from the condenser, thus helping to improve cycle efficiency. Station 6 is the turbine exit vapour, station 7 is the recuperator outlet towards the condenser, station 1 is the inlet of the condensate from the condenser, and station 2 is the pre-heated feed to the preheater.

The heat balance equation between the turbine exit vapour and the condensate is:

$$Q_R = \dot{m}_1(h_6 - h_7) = \dot{m}_6(h_2 - h_1) \tag{13}$$

where Q_R = Heat transfer through recuperator; and
$\dot{m}_1 = \dot{m}_6 = \dot{m}_{fluid}$ = mass of working fluid.

The mass flow is the same on both sides of the regenerator. The hot vapour coming from the turbine is condensed in the condenser and then pumped through the recuperator towards the preheater. It must be observed that the temperature of the hot vapour is higher than that of the cold fluid throughout the recuperator. Fluid behaviour is usually close to linear.

When regeneration is used, plant efficiency increases and plant effectiveness is reduced. It increases the temperature of the working fluid at the preheater entry, and thus leads to higher geothermal fluid exit temperature from the preheater. In a geothermal unit, regeneration increases the thermal efficiency of the cycle.

5.4.5 Air cooled condenser

The function of the condenser is to condense the exhaust low-pressure vapour flowing from the turbine. The condenser may be water, air or spray cooled. Keeping in mind the climatic conditions and insufficient water availability in the area, an air cooled condenser was selected for the above proposed binary cycle. An air-cooled condenser (Figure 15) is a fin-fan type heat exchanger in which low-temperature vapour coming from the turbine outlet passing through a regenerator is condensed by transferring heat to the surrounding air, blown by the fans to the condenser. In the air-cooled condenser, the air temperature difference in the cooling tower is between 12 and 14°C, and the resulting working fluid temperature is about 40°C (Páll Valdimarsson, pers. comm.).

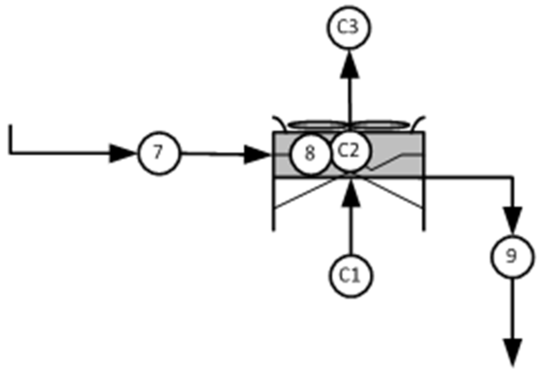

FIGURE 15: Air cooled condenser

Station 7 is the working fluid coming from the recuperator. Station 9 is the condensed fluid, normally saturated liquid with little or no sub-cooling. Station c1 is the entry of the cooling fluid (ambient air), station c3 is the outlet of the air.

The heat that is rejected by the working fluid to the cooling medium (ambient air) is given by:

$$Q_C = \dot{m}_a c_p \, \Delta T_{cooling} = \dot{m}_{fluid} \, (h_7 - h_9) \tag{14}$$

The relationship between the flow rates of the working fluid and the cooling medium is:

$$\dot{m}_a(h_{c3} - h_{c1}) = \dot{m}_{fluid}(h_7 - h_9) \quad (15)$$

where Q_C = Heat transfer through condenser;
$\dot{m}_a$ = Mass of the air.

To calculate the power of the fan:

$$W_{fan} = \frac{v_a \, \Delta p}{\eta_{fan}} \quad (16)$$

$$v_a = \frac{\dot{m}_a}{\rho_{a,out}} \quad (17)$$

$$P_{fan,motor} = \frac{P_{fan}}{\eta_{fan,motor}} \quad (18)$$

where Δp = Pressure drop (Pa);
v_a = Volume flow rate of air (m^3/s);
$\dot{m}_a$ = Mass flow rate of air (kg/s);
$\rho_{a,out}$ = Density of air (kg/m^3);
η_{fan} = Efficiency of fan.

5.4.6 Feed pump

The power imparted to the working fluid by the feed pump (Figure 16) is given as:

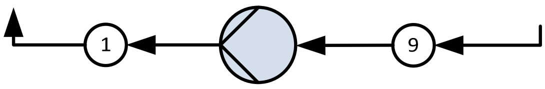

FIGURE 16: Feed pump

$$W_{fp} = \dot{m}_{fluid}(h_7 - h_9) \quad = \dot{m}_{fluid}(h_{7s} - h_9)/\eta_p \quad (19)$$

where W_{fp} = Work done by the feed pump;
η_p = Isentropic pump efficiency.

5.4.7 Preheater

The preheater (Figure 17) receives the geothermal fluid (at station s6) coming from the outlet of the regenerator to heat the working fluid coming from the feed pump to a saturated liquid state. The minimum temperature difference between the entering geothermal fluid and the leaving working fluid is called the "pinch point" and the value of that difference is designated as the pinch-point temperature difference. The geothermal fluid leaves the preheater at station s7.

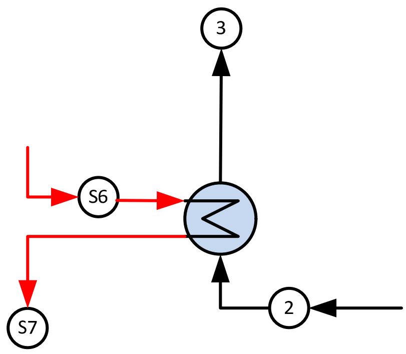

FIGURE 17: Preheater

The preheater provides sensible heat to raise the working fluid to its boiling point, station 3. The heat losses in the heat exchanger are neglected; the amount of heat added to the working fluid is equal to the heat extracted from the geothermal fluid:

$$\dot{m}_{s6}(h_{s6} - h_{s7}) = \dot{m}_{fluid}(h_3 - h_2) \quad (20)$$

Since a constant heat capacity of the geothermal fluid is assumed, enthalpy difference may be replaced by temperature difference:

$$Q_{Ph} = \dot{m}_{s6} \, c_g(T_{s6} - T_{s7}) = \dot{m}_{fluid}(h_7 - h_9) \quad (21)$$

where Q_{Ph} = Heat transfer through preheater;
c_g = Specific heat of geothermal fluid at constant pressure.

5.4.8 Evaporator

The evaporator (Figure 18) receives the geothermal fluid from the outlet of the super-heater and provides the heat of vaporisation for the working fluid coming from the preheater, thus bringing it from a saturated liquid at boiler pressure; the station 4 is a saturated vapour state. The evaporation occurs from 3 to 4 along an isotherm for a pure working fluid. The working fluid in its vapour state is fed to the superheater. The energy balance equation in the evaporator is given as:

$$Q_E = \dot{m}_{s3}(h_{s3} - h_{s4}) = \dot{m}_{fluid}(h_4 - h_3) \tag{22}$$

where Q_E = Heat transfer through evaporator.

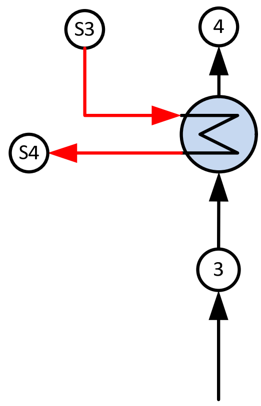

FIGURE 18: Evaporator

5.5 Net power output of the cycle

The net power of the cycle is calculated as follows:

$$\dot{W}_{net} = \dot{W}_t - \dot{W}_{fp} - \dot{W}_{fan} \tag{23}$$

6. HEAT DISSIPATION FOR A BINARY CYCLE

The heat dissipation system is of great importance for binary power plants because of significantly bigger quantities of rejected heat per unit of electricity output, compared to fossil or nuclear power plants, as well as high sensitivity for temperature variations of the heat sink. The heat dissipation from the cycle is primarily a heat of condensation of the working fluid and it can be defined in terms of the thermal efficiency of the cycle as:

$$Q_{rej} = Q_{in}(1 - \eta_{th}) \tag{24}$$

where Q_{in} = Heat input to the cycle, in this case, it is the sum of heat rates of the preheater, evaporator and superheater;
η_{th} = Thermal efficiency of the cycle.

The amount of heat that has to be rejected to the atmosphere per unit of work output is:

$$Q_{rej} = W_{net}\frac{1 - \eta_{th}}{\eta_{th}} \tag{25}$$

Because of low thermal efficiency of ORC running on low quality heat sources, the amount of waste heat per unit of work is approximately 5-7 times greater than from the average fossil fuel power plant (Kestin et al., 1980). On the other hand, the heat dissipation system in binary units has a tremendous effect on cycle efficiency. The Carnot efficiency term $\eta_{th} = \frac{T_1 - T_0}{T_1}$ shows that the lower the temperature of the heat sink becomes, the bigger the effect on cycle performance from a change in sink temperature.

There are several solutions for waste heat rejection systems in binary power plants, two of them are the most popular among commercially available systems: the mechanical-draft cooling tower and the air cooled condenser. Weather conditions and availability of water are crucial parameters determining the choice between the two systems. Water cooled systems are generally considered less expensive to build and operate as long as makeup water is available and cheap. Although in some arid areas plants using air-cooled condensers may be more cost-effective, their power capacity is highly dependent on weather conditions and their net power output usually fluctuates between 20 and 25% (Geothermal Energy Association). Power plants equipped with air-cooled condensers reach a higher power output at night, when demand for electricity is lower. Using a wet cooling tower, a working fluid can be cooled down to lower temperatures, which improves the efficiency of the cycle significantly.

In Puga, the availability of water is inconsistent. It varies from 250 l/s in summer to 25 l/s in winter. The winter season in this area lasts for about 6-7 months and winds blow at a speed of about 4 km/hr to more than 10 km/hr. Keeping in mind the weather conditions, the air-cooled condenser was chosen for the proposed power cycle.

Calculation of thermal efficiency for the cycle
η_{th} stands for thermal efficiency of the cycle. According to the first law of thermodynamics, the thermal efficiency is given as:

$$\eta_{th} = \frac{W_{net}}{Q_{in}} \tag{26}$$

In the above equation, the thermal efficiency obtained will not be the exact value as it only uses the heat input at heat exchangers. However, in the above proposed binary cycle, the thermal efficiency is calculated in the EES programme as shown below:

$$\eta_{th} = \frac{W_{\_dot\_net}}{Q_{available}} \tag{27}$$

where $W_{\_dot\_net} = W_{\_dot\_turbine} - W_{\_dot\_parasitic\_power}$, and
$W_{\_dot\_parasitic\_power} = W_{\_dot\_pump} + W_{\_dot\_fanmotors}$

Parasitic power is the power consumed by the power plant equipment such as pump motors and fan motors, and $Q_{available}$ is the heat available at the wellhead and is calculated by the following equation:

$$Q_{available} = \dot{m}_{s1}(h_{s1} - h_{s,minimum}) \tag{28}$$

where $h_{s,minimum}$ = Enthalpy (water, $T = T_{c1}$, x = 0);
T_{c1} = 10°C (value assumed for ambient air temperature); and
$\dot{m}_{s1}$ = Mass flow rate at the wellhead.

In case of binary power plants, thermal efficiencies lie in the range of 10-13% (DiPippo, 2008).

7. REINJECTION TEMPERATURE

Reinjection is a very vital part of any geothermal development and may become the key factor in the success or failure of the field. Reinjection started as a method for waste water disposal, but now it has become an important tool for field management (Eylem et al., 2011).

In order to achieve maximum conversion of geothermal energy into electricity, the geothermal fluid must be cooled to as low as possible. In many cases, the geothermal fluid becomes supersaturated with silica as it is cooled. A hotter resource temperature will lead to higher silica saturation in the disposal brine, the consequences of which could lead to greater silica scaling precipitation in reinjection wells, piping, heat exchangers and other production facilities (DiPippo, 1985).

8. SCALING AND ITS PREVENTION

The decrease in temperature of geothermal water during utilization has a dangerous effect on the solubility in the system leading to supersaturation and resulting in scale depositions. The type of scaling depends on the chemical composition of the geothermal water, the temperature of the water and the composition of the distribution system material. In intermediate- and low-temperature geothermal systems, calcium carbonate scaling has been reported by a few authors. Vuataz et al. (1989) dealt with calcite saturated waters in the sandstone aquifer at Melleray, France, where a combination of sulphide and calcite scale was responsible for the deterioration of reinjection well permeability. Kristmannsdóttir (1989) also noted that calcite scale was encountered in low-temperature systems in Iceland when fluids were allowed to degas and, on occasion, when fluids of different temperatures or salinities were allowed to mix. Prevention of scale deposition in low-temperature systems is typically controlled by limiting the extent of degassing and the resultant pH changes that bring about the supersaturation of carbonate minerals.

Two of the most common geothermal scales are silica (SiO_2) and calcite ($CaCO_3$). Both these scales are white in colour and are not easy to tell apart visually. Silica is found in most geothermal fluids in different concentrations, generally increasing with higher reservoir temperatures. The silica scales often appear grey or black due to small amounts of iron sulphide, a corrosion product found inside all geothermal pipelines. A quick method for distinguishing between the two is to put a drop of hydrochloric acid on a piece; if bubbles form, it is calcite (Thórhallsson, 2005).

8.1 Scale prevention

At supersaturated conditions, silica and metal silicates take some time to equilibrate. The reactions are strongly influenced by pH, temperature and salinity. The lower values slow down the scaling rate of silica and this is often taken advantage of in process design. An example of this is the acidification of silica supersaturated solutions to lower the pH sufficiently (to approximately pH 4.5-5.5) to slow down scale formation, for example in the heat exchanger of binary units. This may increase the corrosion rate in the pipeline. It is relatively simple to inject sulphuric acid or hydrochloric acid, by means of a chemical metering pump, into the brine pipeline (Thórhallsson, 2005).

By rapidly dropping the brine temperature on the second flash separator, for example by the use of a vacuum, scaling is much reduced. Then second flash steam can be used and the waste brine will leave the processing equipment without clogging it. Saline solutions will precipitate silica more quickly than dilute solutions, due to a higher reaction rate. Thus, the slow scaling rate in dilute geothermal water can be taken advantage of and binary units can be operated within scaling regimes, which is not possible with brines. To reduce silica concentration and keep a high enough temperature before reinjection, mixing between brine and condensate is a good idea, as experienced in some fields like in the Svartsengi plant in Iceland (Thórhallsson, 2012).

The scaling condition constantly changes as the geothermal fluid travels from the wells and through the pipelines and back to the reservoir. This makes scaling prediction somewhat uncertain but, by combining chemical modelling calculations, pilot studies and practical experience, it has usually been possible to come up with solutions that will overcome the most serious scaling problems. To monitor scaling or corrosion at various locations in the pipelines, it is possible to install retractable coupons that can be removed for periodic inspection without affecting the flow or operation of the plant (Thórhallsson, 2005).

8.2 Scale removal

There are different types of scale removing methods. Selection of method is dependent on the cost of the method and the required time, especially if the plant has to be out of operation (Thórhallsson, 2012):

1. *Chemical removal method*
   The chemical method includes the use of either acid (acidizing) or base to dissolve an existing scale. The chemical cleaning method has some advantages over the mechanical cleaning method.

One advantage is that pipes or other equipment do not need to be disassembled and reassembled. Acid removes deposits from the surface.

2. *Mechanical removal method*
   Mechanical cleaning includes scraping and scratching to clean deposits from the walls or casing of a well and from pipelines. In a well, a scratcher or reamer is lowered into the bore and deposits are removed by the simultaneous rotary transverse motion of the reamer. Reaming is an expensive method for scale removal. Scraping can be used to remove scale formed in pipelines by running scrapers (sometimes referred to as pipe pigs) through the lines at regular time intervals. These are inserted and removed at inlet and outlet traps.
3. *Hydro blasting method*
   Application of a water jet to remove scale is a common method applied at geothermal power plants. One scale removal method employs pulsating high-pressure jets of water which are directed against the scale surface.

9. MODEL CALCULATIONS

9.1 Calculations of heat exchanger area

The area and heat transfer of the preheater, evaporator, superheater and condenser were calculated using the following formula after putting the values into the EES programme:

$$Q = UA \times LMTD \tag{29}$$

where U = Overall heat transfer coefficient (°C/m^2);
A = Heat transfer area (m^2); and
$LMTD$ = Log mean temperature difference (°C) which is calculated as:

$$LMTD = \frac{(T_{hot,in} - T_{cold,out}) - (T_{hot,out} - T_{cold,in})}{\ln\left[\frac{T_{hot,in} - T_{cold,out}}{T_{hot,out} - T_{cold,in}}\right]} \tag{30}$$

The values of the heat transfer and area of the heat exchangers calculated in EES for the selected working fluids are shown in Table 3.

TABLE 3: Values for heat transfer and area of heat exchangers for selected working fluids

No.	Working fluid	Q_{regen} (kJ/kg)	$Q_{superheater}$ (kJ/kg)	$Q_{preheter}$ (kJ/kg)	Q_{Evap} (kJ/kg)	$Q_{condenser}$ (kJ/kg)	$A_{Recuperator}$ (m^2)	$A_{superheater}$ (m^2)	$A_{preheater}$ (m^2)	A_{Evap} (m^2)	$A_{Condenser}$ (m^2)
1	Isobutane	1851	1117	21615	49641	26697	1108	493.3	16814	6200	6867
2	n-butane	14218	1159	38656	49600	73757	1108	282	16814	6200	6867
3	Isopentane	14218	1159	38656	49600	73757	1108	493.3	16814	6200	6867
4	n-pentane	12844	955.8	35365	49803	70972	1009	406.9	7864	6225	6598
5	Propane	The pressure and temperature went above their critical limit.									

9.2 Cost estimation of the model

Capital cost of geothermal projects are very site and resource specific. The resource temperature, depth, chemistry and permeability have major effects on the cost of the power project. The resource temperature will determine the power conversion technology (steam and brine) as well as the overall efficiency of the power system. Site accessibility, topography, local weather conditions, land type and ownership are additional parameters affecting the cost and the time required to bring the power plant online. The base cost of main equipment are estimated based on the experience of experts as shown in Table 4. In this study the costs assumed are thumb values. The cost of components of the binary cycle based on the working fluid, which in this case is isopentane, is shown in the table below.

TABLE 4: Assumed thumb values for costs of equipment for model binary cycle with n-pentane as working fluid

S.no.	Equipment	Unit size	Basic cost /unit size (USD/m^2, kW)	Area of the equipment (m^2)	Cost of equipment (USD)
1	Preheater	m^2	450	16814	756,300
2	Evaporator	m^2	500	6200	3,100,000
3	Superheater	m2	500	493.3	246,650
4	Recuperator	m^2	400	1108	443,200
5	Condenser	m^2	600	73757	44145000
6	Turbine	kW	500	14847	7423,500
7	Pump	kW	450	539.6	242,820

The cost of piping in the power plants is usually in the range of 10-70% of the purchased equipment cost (PEC). Although it is suggested that for plants handling fluid and with heat recuperators the higher numbers in this range apply, for geothermal power plants the relative cost of pipes is much lower. It is caused by lower piping diameters and the high cost of other components in binary units. The cost of pipes in this range (5-75 cm) is almost linearly dependent on their diameters (Bejan et al., 1988), therefore the total cost of piping is assumed to be equal to 7% of PEC for geothermal applications and 9% of PEC for waste heat recovery systems.

9.3 Calculation results

Detailed calculations and optimisation work for different working fluids were carried out using programming done with Engineering Equation Solver software. The diagram of the model binary cycle with EES values is shown in Figure 19. The system parameters used in this work are mentioned in Sections 5.1 and 5.2. The main results of each working fluid are summarized in Table 5.

TABLE 5: Summary of calculated power output

S.no.	Working fluids	Net output (kW)	Thermal efficiency (%)	Turbine inlet pressure (bar)	Reinjection temperature (°C)	Mass flow of working fluid (kg/s)
1	isopentane	14847	11.54	12.77	72.59	212.1
2	isobutane	10855	8.434	32.28	48.81	200.4
3	n-pentane	14373	11.17	10.71	77.82	192.3
4	n-butane	13998	10.88	25.68	54.47	212.13

After putting the above values into the EES programme, results were obtained for different working fluids. As per the objective to gain optimum power output, the results obtained are shown in Figure 20. It was found that isopentane meets our demand, giving the highest net power output of approximately 15 MW.

It is clear that the isobutane produces the lowest net power output and lowest reinjection temperature, i.e. the lowest district heating capacity in contrast with other working fluids. The highest net power output was obtained from the isopentane working fluid, having also a reasonable district heating capacity supply because of a reinjection temperature of 72.59°C. In the case of n-pentane, the net power output had the higher value as well as a good district heating capacity supply. Even though Scenario 4 gave the highest value in thermal efficiency, and a good net power output, it had very little district heating capacity. Since the reinjection temperature in the proposed model is high, a scaling problem is not likely to be encountered in the reinjection wells.

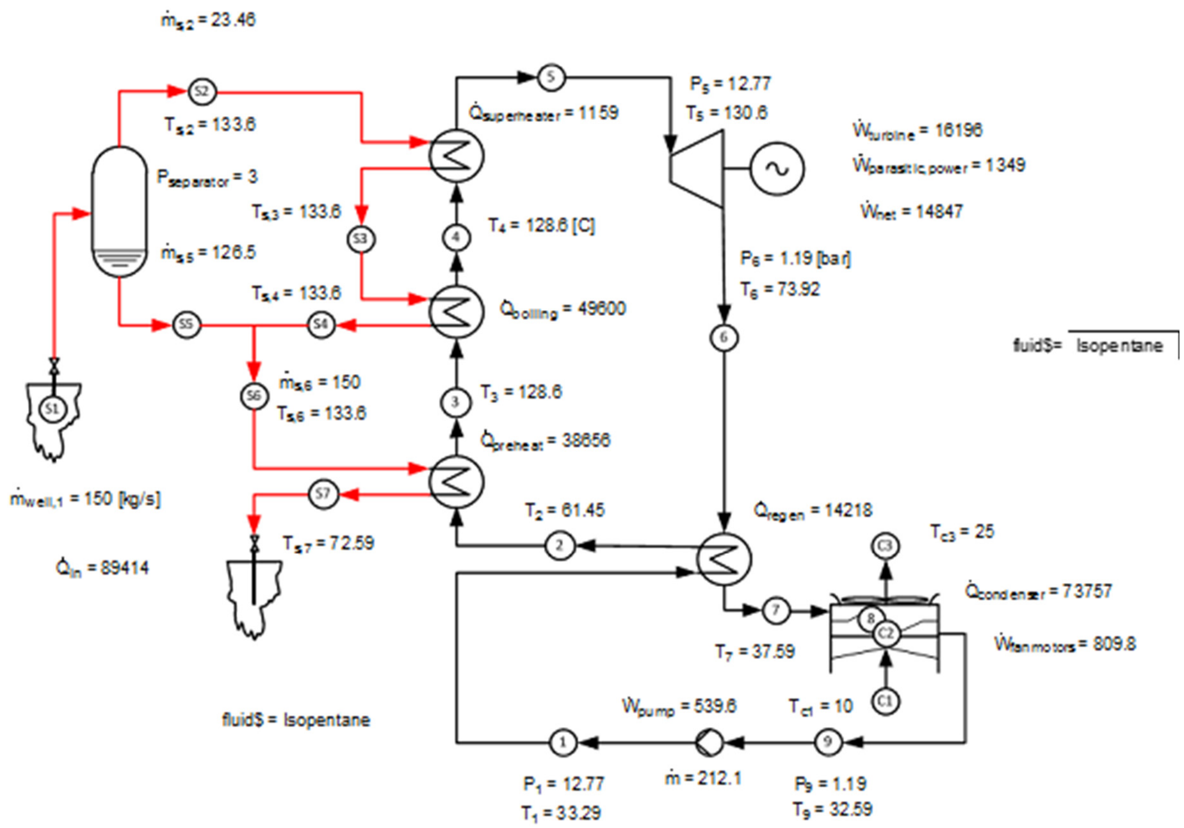

FIGURE 19: Schematic diagram of proposed binary plant with EES values, isopentane as working fluid

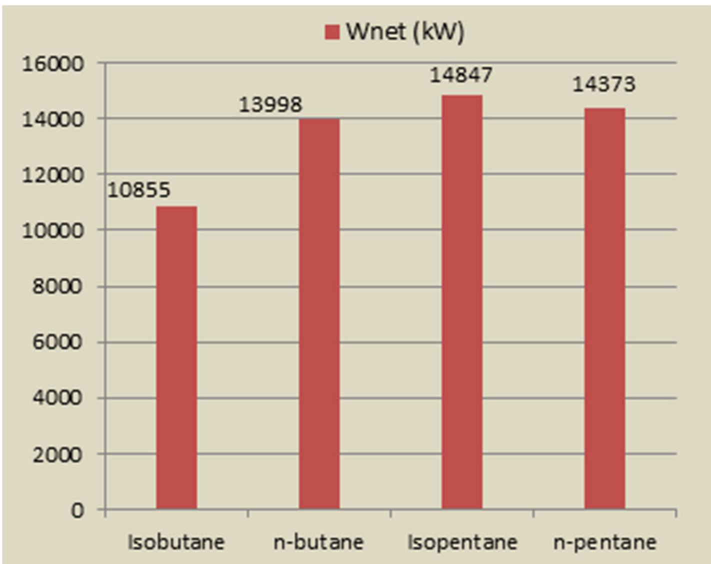

FIGURE 20: Net optimum output of the plant

10. CONCLUSIONS

Production of electricity would be economically unjustified without a properly chosen working fluid in a binary cycle according to the thermodynamic parameters of the geothermal fluid. The proposed cycle described in this paper utilises a geothermal heat source containing steam and brine, where enthalpy and wellhead pressure is relatively low.

Based on the energy assessment in Puga, a proposed binary power cycle was designed to investigate the technical feasibility. It was shown that such a design was sensible. The highest power generated by the turbine was obtained when isopentane was used as the working fluid. The highest requirement of parasitic power of systems using isopentane and n-butane is a result of bigger heat input to the cycle. Among all the working fluids investigated, isopentane assured the best performance.

In this paper, the performance of a binary power cycle with a recuperator was also analysed. In geothermal power plants, the use of a recuperator allows a reduction in the size of the preheater and evaporator. Since these two heat exchangers are manufactured from expensive stainless steel, the effect of such a change on the cost of the unit is significant, compensating partly for the cost increase of the recuperator. The recuperated binary cycle does not increase the net power produced, but increases the plant return temperature, resulting in less danger of scaling, and/or making district heating more feasible.

The main conclusion is that a recuperated binary cycle with isopentane as a working fluid is the most feasible of the cycles studied. There are indications that a hybrid steam – binary cycle may have even better performance, but a study of such a cycle was out of the scope of this work.

The main aim behind the construction of a binary plant and its utilization in the Puga area is not only to produce renewable energy at a reasonable cost, but also an effort to improve the local people's living standards and quality of life.

ACKNOWLEDGEMENTS

I take great pleasure in giving special thanks to Dr. Ingvar B. Fridleifsson, Director of UNU-GTP, for providing me the opportunity to join this valuable six months training programme and to Mr. Lúdvík S. Georgsson, Deputy Director, for providing all facilities and support throughout the entire training period. My thanks go to Mr. Ingimar G. Haraldsson, Ms. Málfrídur Ómarsdóttir and Mr. Markús A.G. Wilde for their cooperation and support. My thanks also go to Ms. Thórhildur Ísberg for her great care and guidance during my stay in Iceland. I am also thankful to the staff of the ISOR library for providing valuable books required during the training.

My sincere thanks go to my supervisor Dr. Páll Valdimarsson for his guidance and constant supervision during the entire project period. Thanks to all the lecturers from UNU-GTP, ISOR, University of Iceland for sharing their valuable knowledge and experience on geothermal science.

I feel great honour and privileged to express my gratitude to Shri Omar Abdullah, Chairman J&K State Power Development Corporation and to Shri Basharat Ahmed Dhar, Managing Director, JKSPDC, for granting me permission to undergo this training at UNU-GTP, Reykjavik, Iceland. I am obliged to Shri Iftikhar Ahmed Kakroo, Deputy General Manager, JKSPDC, for his support. To me, he has always been a source of inspiration.

Last, but not least, my deepest sense of appreciation to my family, especially to my dear father, my mother, my beloved wife, daughter Muntaha and nephew Ziyan for all their sacrifice, moral as well as emotional support, patience and their prayers which helped me in accomplishing this training.

REFERENCES

Absar, A., 1981: *Report on Puga Chhumathang geothermal exploration project*. Geological Survey of India – GSI, report for field season 1980-81.

Bejan, A., Tsatsaronis, G., and Moran, M., 1996: Thermal design and optimization. John Wiley & Sons, Inc., NY, 542 pp.

DiPippo, R., 1985: A simplified method for estimating the silica scaling potential in geothermal power plants. *Geothermal Resources Council, Bulletin*, *May*, 3-9.

DiPippo, R., 2008: *Geothermal power plants. Principles, applications, case studies and environmental impact.* Elsevier Ltd., Kidlington, UK, 493 pp.

Eylem, K., Zarrouk, S.J., and O'Sullivan, M.J, 2011: Reinjection in geothermal fields: A review of worldwide experience. *Renewable and Sustainable Energy Reviews, 15*, 47-68.

F-Chart Software, 2012: *EES, Engineering equation solver.* F-Chart Software, website: *www.fchart.com/ees/ees.shtml.*

Giggenbach, W.F., 1986: Graphical techniques for the evaluated water/rock equilibration conditions by use of Na, K, Mg and Ca contents of discharge water. *Proceedings of the 8th New Zealand Geothermal Workshop,* 37-43.

GSI, 2008: *Geothermal energy resources and its potential in India.* Geological Survey of India, report.

Harinarayana, T., Abdul Azeez, K.K., Naganjaneyulu, K., Manoj, C., Veeraswamy, K., Murthy D.N. and Prabhakar Eknath Rao, S., 2004: Magnetotelluric studies in Puga valley geothermal field, NW Himalaya, Jammu and Kashmir, India. *J. Volcanol. & Geothermal Res., 138*, 405-424.

Kestin, J., DiPippo, R., Khalifa, H.E., and Ryley, J. (editors), 1980: *Sourcebook on the production of electricity from geothermal energy*. U.S. Dept. of Energy, Washington, D.C., 997 pp.

Kristmannsdóttir, H., 1989: Types of scaling occurring by geothermal utilization in Iceland. *Geothermics, 18*, 183-190.

Mishra, H.P., Ghatak, T.K., Rai, R.P. and Mishra, R.K., 1996: Geoelectrical studies for demarcating reservoir in Puga valley, Ladakh, In: Pitale, U.L. and Padhi R.N. (eds.), *Geothermal energy in India*. Geol. Surv. Ind., Special. Publ., 45, 65-68.

MNRE, 2008: *Report on power generation from geothermal energy at Puga, J&K.* Ministry of New and Renewable Energy, Government of India, report of expert group.

Ravi Shanker, Padhi, R.N., Arora, C.L., Gyan Prakash, Thussu, J.L. and Dua, K.J.S., 1976: Geothermal exploration of the Puga and Chhumathang geothermal fields, Ladakh, India. *Proceedings of the 2nd U.N. Symposium on the Development and Use of Geothermal Resources, San Francisco, 1,* 1245-1258.

Ravi Shanker, 1988: Heat flow map of India and discussions on its geological and economic significance. Indian Miner., 42, 89-110.

Ravi Shanker, Absar, A., Srivastava, G.C., and Pandey, S.N., 1999: Source and significance of anomalously high cesium in geothermal fluid at Puga, Ladakh, India. *Proceedings of the 21st NZ Geothermal Workshop, Auckland, New Zealand*, 79-82.

Srivastava, G.C., Srivastava, R. and Absar, A., 1996: Application of gas chemistry in evaluating reservoir temperature of some Indian geothermal systems. In: Pitale, U.L. and Padhi R.N. (eds.), G*eothermal energy in India*. Geol. Surv. Ind., Special. Publ., 45, 83-86.

Thórhallsson, S., 2005: Common problems faced in geothermal generation and how to deal with them. *Paper presented at Workshop for Decision Makers on Geothermal Projects and Management, organized by UNU-GTP and KenGen in Naivasha, Kenya*, 12 pp.

Thórhallsson, S., 2012: *Problems of geothermal utilization*. UNU-GTP, Iceland, unpublished lecture notes.

Valdimarsson, P., 2011: Geothermal power plant cycles and main components. *Presented at the "Short Course on Geothermal Drilling, Resource Development and Power Plants", organized by UNU-GTP and LaGeo, in Santa Tecla, El Salvador,* 24 pp.

Vuataz, F., Czernochowski-Lauriol, I., Fouillac, C., and Detoc, S., 1989: Chemical study of a low-temperature geothermal fluid in a Triassic sandstone aquifer: Scaling potential and fluid treatment. *Geothermics, 18,* 313-320.